Journal of Magnetism and Magnetic Materials 499 (2020) 166302

Contents lists available at ScienceDirect

Journal of Magnetism and Magnetic Materials

journal homepage: www.elsevier.com/locate/jmmm

Research articles

Enhanced magnetocaloric effect in undercooled rare earth intermetallic compounds RNi (R = Gd, Ho and Er)

Jinu Kurian[a], M.R. Rahul[b], J. Arout Chelvane[c], A.V. Morozkin[d], A.K. Nigam[e], Gandham Phanikumar[b], R. Nirmala[a,*]

[a] Department of Physics, Indian Institute of Technology Madras, Chennai 600 036, India
[b] Department of Metallurgical and Materials Engineering, Indian Institute of Technology Madras, Chennai 600 036, India
[c] Defence Metallurgical Research Laboratory, Hyderabad 500 058, India
[d] Department of Chemistry, Moscow State University, Moscow GSP-2, 119992, Russia
[e] Tata Institute of Fundamental Research, Mumbai 400 005, India

ARTICLE INFO

Keywords:
Rare earth intermetallic compounds and alloys
Magnetic properties
Magnetocaloric effect

ABSTRACT

Equiatomic RNi (where R = Gd, Ho and Er) compounds have been prepared by undercooling. Magnetization data confirm ferromagnetic ordering of the samples at 69 K, 35 K and 10 K (T_C) respectively. Magnetocaloric effect (MCE) has been estimated in terms of isothermal magnetic entropy change (ΔS_m) near T_C. The maximum ΔS_m value (ΔS_m^{max}) for 50 kOe field change is about -18 $Jkg^{-1}K^{-1}$, -20 $Jkg^{-1}K^{-1}$ and -30 $Jkg^{-1}K^{-1}$ respectively near T_C for the undercooled RNi (R = Gd, Ho and Er) compounds. The ΔS_m^{max} value is more than that obtained for the same compounds prepared by arc-melting and melt-spinning techniques. The observed enhancement in MCE of the undercooled samples could be due to the improved purity that results in faster change of magnetization around the magnetic transition. Thus undercooling rare earth intermetallics and alloys seems to be an attractive, alternative method to synthesize magnetocaloric materials.

1. Introduction

Melt-spinning is a non-equilibrium rapid solidification process that is characterized by a high cooling rate of about 10^6 K/s. Melt-spinning technique has been used to obtain highly crystalline $LaFe_{13-x}Si_x$-type giant magnetocaloric materials with superior magnetic properties where porosity of the samples was engineered in order to control magnetic hysteresis and the first-order transition temperature [1]. These results have motivated synthesis of various melt-spun, crystalline intermetallic compounds of type RNi_2, R_2Ni_{17} (where R = Rare earth) and Ni-Mn-In based shape memory alloys [2,3,4]. Recent studies on equiatomic RNi compounds [5–9] prepared by melt-spinning showed interesting magnetic and magnetocaloric properties when compared to their arc-melted analogues [10]. Melt-spinning brought in an additional functionality namely granularity. One of the systems (SmNi) exhibited nanosized grains [8] whereas melt-spun RNi with R = Gd, Tb, Dy, Ho and Er had grains of micrometer size [5,6,7]. Rapid solidification can also be achieved by high undercooling of liquid melt. Pioneered by Fahrenheit, undercooling is one of the synthesis techniques that leads to the stabilization of metastable phases in addition to obtaining equilibrium phases in purer form as this is a containerless process [11,12]. The technique can lead to a different microstructure and can help tailor material properties favourably. The rare earth intermetallic compounds RNi are known for large low temperature magnetocaloric effect [10]. The crystal structure of these compounds changes across the rare earth series from orthorhombic CrB-type (LaNi to GdNi) to orthorhombic FeB-type (DyNi to LuNi and YNi) while TbNi is dimorphic [13]. In these compounds, the magnetism is determined largely by the rare earth ion moment. In the present work, single phase GdNi, HoNi and ErNi compounds have been synthesized by undercooling technique and their magnetic and magnetocaloric properties are studied.

2. Experimental Details

Polycrystlalline RNi (where R = Gd, Ho and Er) compounds were prepared by arc-melting under argon atmosphere starting from stoichiometric amounts of pure elements. About 1 g of arc-melted specimens sealed under a vacuum of 10^{-5} mbar in a quartz tube were used for the undercooling experiment. Two colour infrared pyrometer with an accuracy of ± 5 °C was used to record temperature as a function of time. Using the time–temperature plot, undercooling was calculated as the difference between the liquidus temperature and the nucleation

* Corresponding author.
E-mail address: nirmala@physics.iitm.ac.in (R. Nirmala).

https://doi.org/10.1016/j.jmmm.2019.166302
Received 7 February 2019; Received in revised form 19 November 2019; Accepted 13 December 2019
Available online 14 December 2019
0304-8853/

temperature. The sample was superheated to ~200 °C above the liquidus temperature and then cooled. The liquidus temperatures are about 1280 °C, 1060 °C, and 1100 °C for the GdNi, HoNi and ErNi samples respectively. The reduced number of nucleation sites lowers the probability of solidification near the liquidus point thus enhancing the undercooling. The samples were characterized by powder X-ray diffraction [Cu Kα, Rigaku] at room temperature. The unit cell data were derived from the Rietveld analysis of the X-ray data using Rietan program [14]. Microstructure and sample composition were studied using scanning electron microscopy and energy dispersive analysis of X-rays (SEM-EDAX). DC magnetization has been measured using a commercial SQUID-based vibrating sample magnetometer (MPMS 3, Quantum Design) and a SQUID magnetometer (MPMS XL, Quantum Design) at temperatures (T) from 5 K to 300 K in magnetic fields (H) up to 70 kOe.

3. Results and discussion

Powder X-ray diffraction studies confirm the single phase nature of the undercooled GdNi, HoNi and ErNi compounds. The XRD data show that the undercooled GdNi crystallizes in orthorhombic CrB-type structure (space group *Cmcm*, no. 63, *oC*8), the undercooled HoNi and ErNi compounds crystallize in orthorhombic FeB-type structure (space group *Pnma*, no. 62, *oP*8). The arc-melted and melt-spun analogues also are known to stabilize in same crystal structures [6,7,9]. There is a change of texture when the sample is prepared by conventional arc-melting or rapidly solidified by melt-spinning and undercooling. However, there is only a small change in lattice parameters and unit cell volume [6,7,10]. Typical XRD patterns of undercooled CrB-type and FeB-type RNi compounds are shown in Fig. 1. The (h k l) values of the maximum intensity XRD peaks are listed for all the three compounds prepared by these three different techniques (Table 1 and Fig. 1). The maximum intensity peak is found to occur at different Bragg angles within the FeB-type structure of the Ho and Er-based samples when prepared by a non-equilibrium, rapid solidification process of undercooling and melt-spinning (Table 1). The nature of the rare earth ion such as size, the melting point of the material and the exact solidification conditions of the non-equilibrium synthetic process are expected to play a role in deciding the crystallographic texture.

The ratio of the constituent elements is close to 1:1 in all the three compounds as evidenced in EDAX data. The scanning electron micrographs revealed micron-sized grains in melt-spun RNi (R = Gd, Ho and Er) materials [6,7]. One could not observe such well-defined grains in both the arc-melted and the undercooled samples. However, one should note that the SEM study was attempted on samples that were not chemically etched. One could suppose that the grains of undercooled samples are larger in size (also as evidenced via the sharp Bragg peaks of powder XRD data) than in the corresponding melt-spun analogues where there is substantial broadening. This could be associated with the availability of minimal number of nucleation sites in the undercooling process and the solidification rates. The change in microstructure and grain size could affect the magnetic hysteresis of the samples in their magnetically ordered state.

The temperature dependent magnetization, M(T), of undercooled RNi (R = Gd, Ho, and Er) compounds has been measured in the zero-field-cooled (ZFC) state in 5 kOe field (Fig. 2) confirms that the samples order ferromagnetically at 69 K, 35 K and 10 K (T_C) respectively. The T_C values are more or less the same as in the corresponding arc-melted and melt-spun samples (Table 2). Ferromagnetic transition temperature of the compounds is obtained by plotting dM/dT vs T. Within the ferromagnetically ordered state, the undercooled HoNi depicts a spin-reorientation transition at ~10 K (T_{sr}) as observed in its arc-melted and melt-spun forms [6,15]. Paramagnetic susceptibility is fitted to Curie-Weiss law and effective paramagnetic moment (μ_{eff}) and paramagnetic Curie temperature (θ_p) values are obtained [Table 2]. Positive value of θ_p of all three compounds confirms that the dominant interactions are

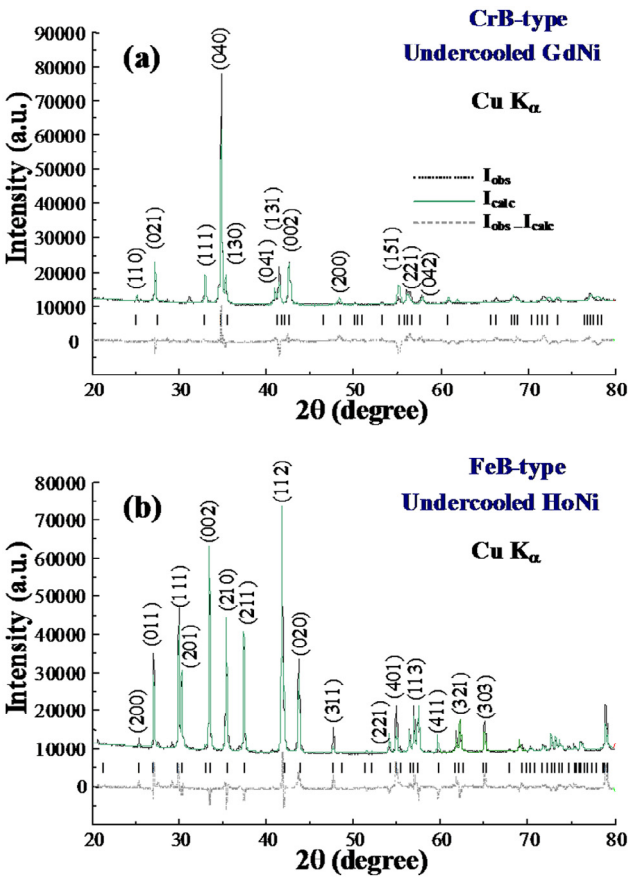

Fig. 1. Powder X-ray diffraction data of the undercooled (a) CrB-type GdNi and (b) FeB-type HoNi compounds and their Rietveld refinement. The corresponding data of arc-melted and melt-spun samples in references [6] and [7] may be referred to for comparison.

ferromagnetic in nature in these materials.

Isothermal magnetization vs field (M-H) data of undercooled RNi (R = Gd, Ho and Er) compounds have been measured at 5 K in fields up to 70 kOe [Fig. 3]. The CrB-type GdNi is known to have a collinear magnetic structure [16] and it saturates in a relatively smaller field of about 15 kOe. Also its saturation magnetization (M_s) value of 7.2 μ_B/f.u. is comparable to the theoretical *gJ* value of 7 μ_B/Gd^{3+}. On the other hand, M_s values of undercooled HoNi and ErNi are only 8.8 μ_B/f.u. and 8 μ_B/f.u. respectively. These are little less than the corresponding theoretical values of 10μ_B/Ho^{3+} and 9μ_B/Er^{3+}. This could be due to the crystal field effects and such reduction in saturation magnetization has also been observed in arc-melted and melt-spun HoNi and ErNi compounds (Table 2). The hysteresis between the virgin and envelope curve of magnetization of HoNi at 5 K is related to the metamagnetic transition observed in this sample [17]. Anisotropic magnetism in HoNi already reported. Neutron diffraction studies on a single crystal of HoNi reveal the existence of antiferromagnetic component along *c* axis from 20 K down to 4.2 K [18]. Field dependent magnetization measurement on single crystal HoNi indeed shows a spin-flop transition when critical field of about 30 kOe is applied along the *c* axis at 5 K [17,19]. The observation of virgin curve lying completely outside the envelope curve at 5 K supports the occurrence of metamagnetism and grain oriented growth in the undercooled HoNi sample. Also it could suggest a field-induced magnetic structure change. The coercivity values of the undercooled samples are intermediate between the values obtained for arc-melted and melt-spun samples. For example, coercivity increases from 0 Oe to 90 Oe for arc-melted to melt-spun GdNi whereas it is only about 21 Oe for the undercooled GdNi sample. This observation agrees with the suggestion from the SEM images of the melt-spun samples that

Table 1
Unit cell data of GdNi (CrB-type, *Cmcm*, N 63, *oC*8), HoNi and ErNi (FeB-type, *Pnma*, N 62, *oP*8) compounds prepared by arc-melting, melt-spinning and undercooling. The (h k l) values of most intense Bragg peak of XRD pattern indicate the texture of the samples.

No.	Compound	Method of preparation	Type structure	*a* (Å)	*b* (Å)	*c* (Å)	*V* (Å^3)	Most intense Bragg peak	R_F (%)
1	GdNi [6]	Arc-melted	CrB	3.7722(3)	10.3100(6)	4.2409(3)	164.93	(1 1 1)	1.2
	GdNi [6]	Melt-spun	CrB	3.7789(5)	10.259(1)	4.2100(6)	163.21	(0 4 0)	1.2
	GdNi *	Undercooled	CrB	3.7653(7)	10.3105(13)	4.2379(11)	164.52	(0 4 0)	3.0
2	HoNi [6]	Arc-melted	FeB	7.0351(8)	4.1487(3)	5.4497(4)	159.06	(2 1 0)	1.8
	HoNi [6]	Melt-spun	FeB	6.9800(3)	4.1106(2)	5.4035(1)	155.04	(0 2 0)	1.7
	HoNi *	Undercooled	FeB	7.0197(3)	4.1398(2)	5.4372(2)	158.01	(1 1 2)	5.4
3	ErNi [7]	Arc-melted	FeB	6.9903(4)	4.1154(2)	5.4163(2)	155.82	(2 0 1)	4.6
	ErNi [7]	Melt-spun	FeB	6.9721(7)	4.1202(5)	5.4222(4)	155.76	(1 0 2)	7.9
	ErNi *	Undercooled	FeB	7.0098(5)	4.1142(3)	5.4256(3)	156.47	(2 1 1)	6.2

* This work.

the smaller size grains in those samples lead to the increased coercivity values because of enhanced domain wall pinning.

Magnetocaloric effect of the undercooled RNi (R = Gd, Ho and Er) compounds has been estimated using the M-H isotherms measured at various temperatures around T_C (Fig. 4a–c). Isothermal magnetic entropy change (ΔS_m) is calculated using the following expression [20]

$$\Delta S_m = \mu_0 \int_{H_i}^{H_f} \left(\frac{\partial M}{\partial T}\right)_H dH$$

where H_i and H_f are the initial and final values of the applied magnetic fields and μ_0 the permeability of free space. The calculated ΔS_m values are plotted as a function of temperature for various magnetic field changes for the undercooled GdNi, HoNi and ErNi compounds (Fig. 5a–c). Isothermal magnetic entropy change attains the maximum value near ferromagnetic transition temperature of each sample and then decreases on either side of peak as expected for a second order transition. The maximum isothermal entropy change, ΔS_m^{max}, of undercooled samples are comparatively larger than that of the corresponding arc-melted and melt-spun samples for a given magnetic field change (Table 3). For example, for 50 kOe field change, ΔS_m^{max} value of undercooled ErNi is about -30 Jkg^{-1}K^{-1} whereas values of -27 Jkg^{-1}K^{-1} and -24 Jkg^{-1}K^{-1} are obtained for the arc-melted and melt-spun ErNi samples. The maximum isothermal entropy change values of

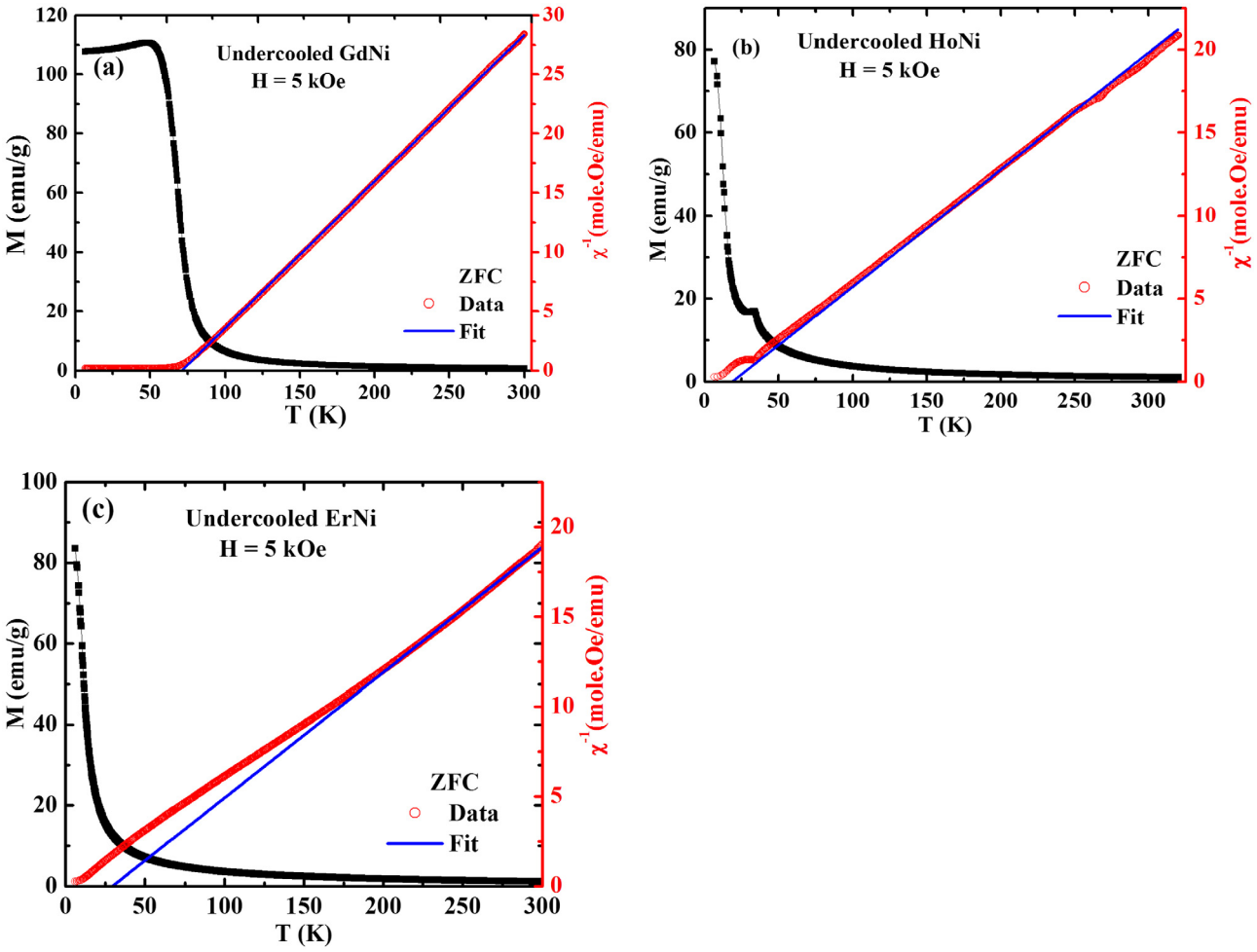

Fig. 2. Magnetization vs temperature of the undercooled (a) GdNi (b) HoNi and (c) ErNi compounds measured in 5 kOe field in zero-field-cooled (ZFC) state while warming. Paramagnetic susceptibility and its fit to Curie-Weiss law is also shown.

Table 2
Details such as ferromagnetic transition temperature (T_C), effective paramagnetic moment (μ_{eff}), paramagnetic Curie temperature (θ_p), saturation magnetization (M_s) and coercivity (H_c) values for the undercooled RNi (R = Gd, Ho and Er) compounds. The data for the corresponding arc-melted and melt-spun samples are also given for comparison.

Compound	T_C (K)	θ_p (K)	μ_{eff} (μ_B/f.u.)	Ms (μ_B/f.u.)	H_c (Oe)	Refs.
Arc-melted GdNi	69	84	8.3	7.4	0	[6]
Melt-spun GdNi	75	85	8.6	7.9	90	[6]
Single crystal GdNi	69	72	8.3	7.2	NA	[23]
Undercooled GdNi	69	65	8.0	7.2	21	This work
Arc-melted HoNi	36	29	10.4	9.2	90	[6]
Melt-spun HoNi	28	12	10.6	8.7	400	[6]
Undercooled HoNi	35	19	10.7	8.8	112	This work
Arc-melted ErNi	11	8	9.8	7.2	62	[7]
Melt-spun ErNi	10	10	9.5	7.4	480	[7]
Undercooled ErNi	10	28	10.7	8.0	56	This work

NA-Not available.

undercooled samples are even better than that of the arc-melted samples which were annealed for several days (Table 3). The ΔS_m^{max} value of undercooled GdNi is −18 J/kg K while it is −17 J/kg K for annealed sample of arc-melted GdNi [9]. Thus the enhancement in the magnetocaloric effect of the undercooled RNi could be attributed to the improved sample purity that is achieved from the preparation conditions that minimize interstitial impurities such as C, N and O. This could enable increased rate of change of magnetization at T_C of the undercooled samples.

The ΔS_m^{max} value for all three undercooled RNi compounds is proportional to $(\Delta H)^n$ with n value as 0.67 for GdNi, 0.68 for ErNi and 0.83 for HoNi, while the mean-field value is 2/3 [21,22] (Fig. 6). The deviation from the mean-field value could be due to the presence of competing magnetic interactions in HoNi and ErNi that have a non-collinear magnetic structure. The relative cooling power (RCP) is the amount of thermal energy transferred by unit mass of the substance from cold sink (T_{cold}) to the hot reservoir (T_{hot}) during one refrigeration cycle and is calculated as a product of magnitude of ΔS_m^{max} and full-width at half maximum (FWHM) of the ΔS_m vs T curve. The T_{hot} and T_{cold} values are ~88 K and 57 K for GdNi and are ~22 K and 7 K for ErNi. The RCP values calculated for the undercooled samples are found to be comparable to that of the arc-melted and melt-spun samples (Table 3). Therefore, in addition to the conventional arc-melting method, melt-spinning and undercooling emerge as alternate synthetic techniques that affect the microstructure of the rare earth intermetallic compounds and hence the magnetic properties. Observation of such enhanced magnetocaloric effect in the undercooled RNi (R = Gd, Ho and Er) compounds motivates one to synthesize other well-known magnetocaloric materials by this method in order to gain a better understanding of process-dependent properties.

4. Conclusions

To summarize, textured intermetallic compounds RNi (R = Gd, Ho and Er) have been synthesized by undercooling technique and their magnetic properties are studied. These samples undergo ferromagnetic ordering at 69 K, 35 K and 10 K as their arc-melted analogues. The synthesis conditions of undercooling technique seem to favour enhancement in the isothermal magnetic entropy change value around the ferromagnetic transition temperature.

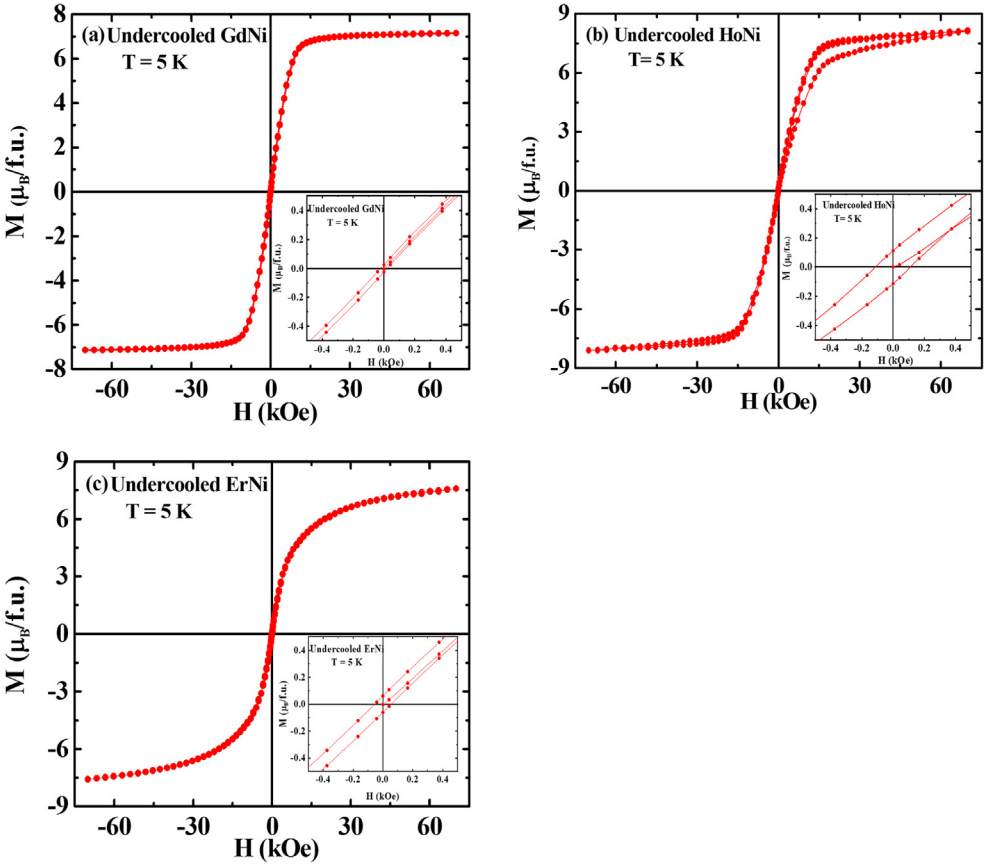

Fig. 3. Magnetization vs field of the undercooled (a) GdNi (b) HoNi and (c) ErNi compounds at 5 K measured in fields up to 70 kOe. Inset shows the low field hysteresis.

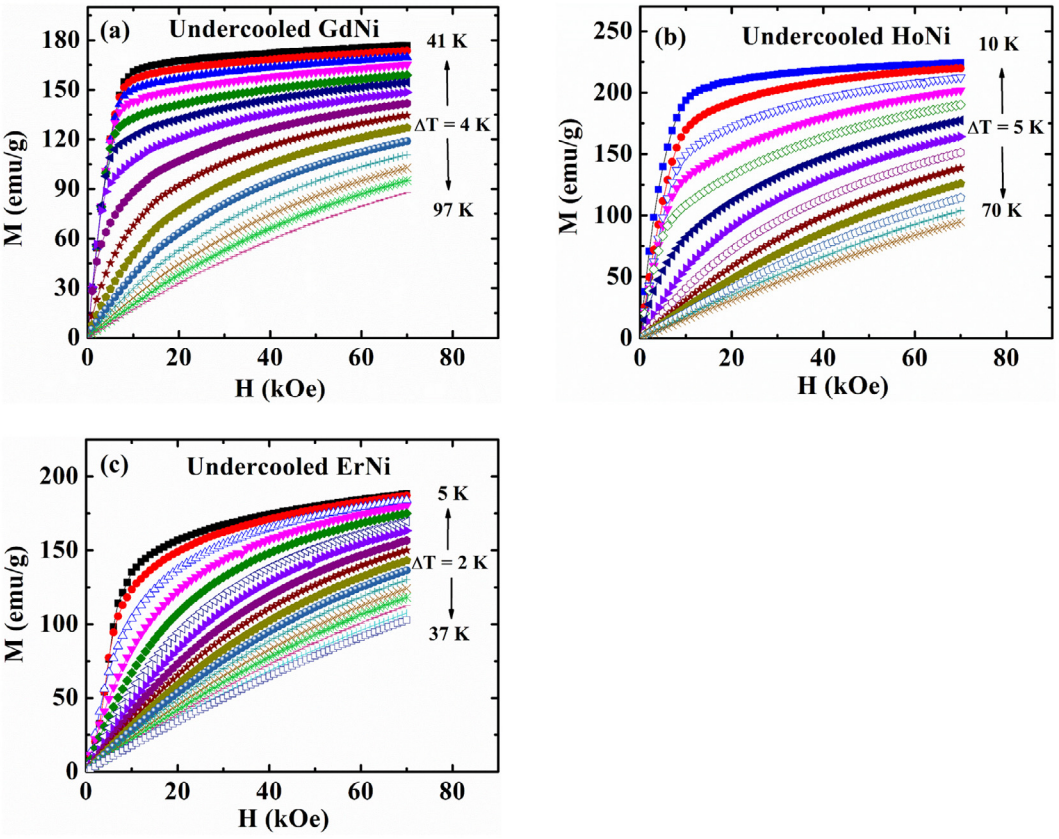

Fig. 4. Magnetizaton vs field isotherms of the undercooled (a) GdNi (b) HoNi and (c) ErNi compounds around the magnetic transition temperature.

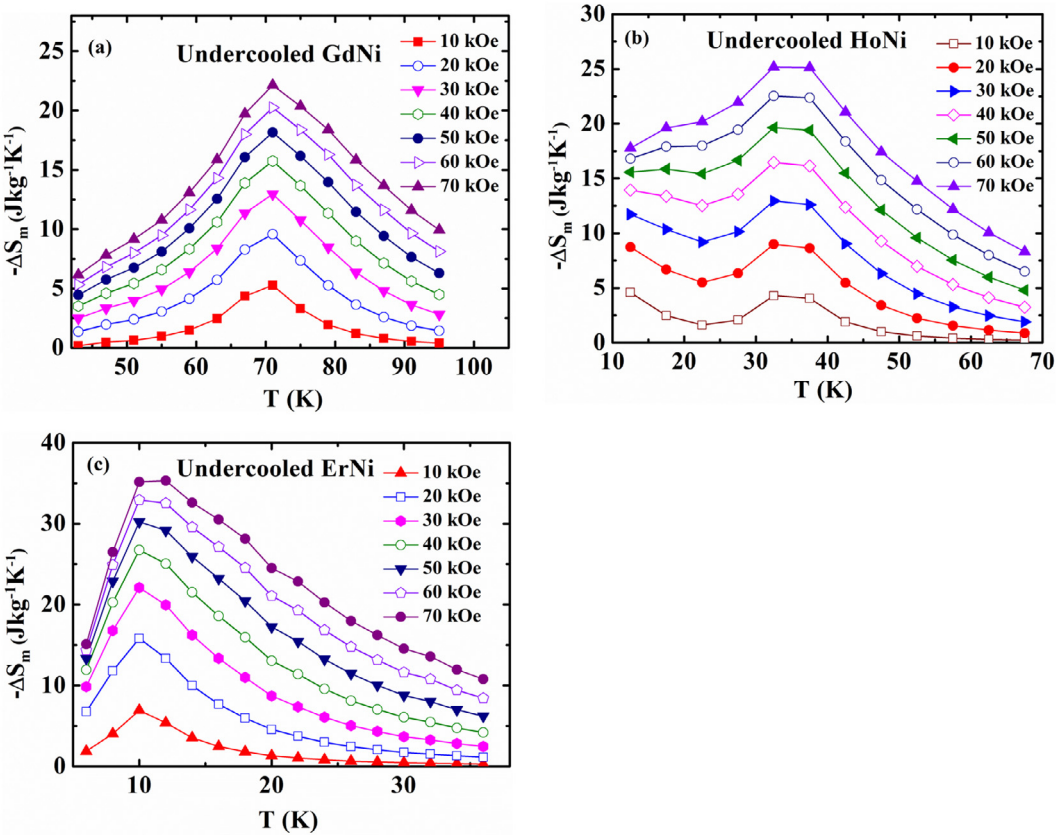

Fig. 5. Isothermal magnetic entropy change (ΔS_m) vs temperature of the undercooled (a) GdNi (b) HoNi and (c) ErNi compounds for various magnetic field changes.

Table 3
Maximum isothermal magnetic entropy change (ΔS_m^{max}) and relative cooling power (RCP) values of the undercooled RNi (R = Gd, Ho and Er) compounds for typical magnetic field changes. For comparison, the corresponding values are listed for the arc-melted and melt-spun compounds from the literature.

Compound	$-\Delta S_m^{max}$ ($Jkg^{-1}K^{-1}$)		RCP (J/kg)		Refs.
	0–20 kOe	0–50 kOe	0–20 kOe	0–50 kOe	
Arc-melted GdNi	9	17	188	575	[6]
Arc-melted GdNi (Annealed)	9	17	180	527	[10]
Melt-spun GdNi	7	15	197	610	[6]
Undercooled GdNi	10	18	188	587	This work
Arc-melted HoNi	8	17	164	750	[6]
Arc-melted HoNi (Annealed)	7	15	330	780	[10]
Melt-spun HoNi	6	14	204	550	[6]
Undercooled HoNi	9	20	#	#	This work
Arc-melted ErNi	14	27	160	440	[7]
Arc-melted ErNi (Annealed)	15	29	300	510	[10]
Melt-spun ErNi	12	25	133	432	[7]
Undercooled ErNi	16	30	149	483	This work

#Could not be calculated because of the low temperature spin-reorientation transition.

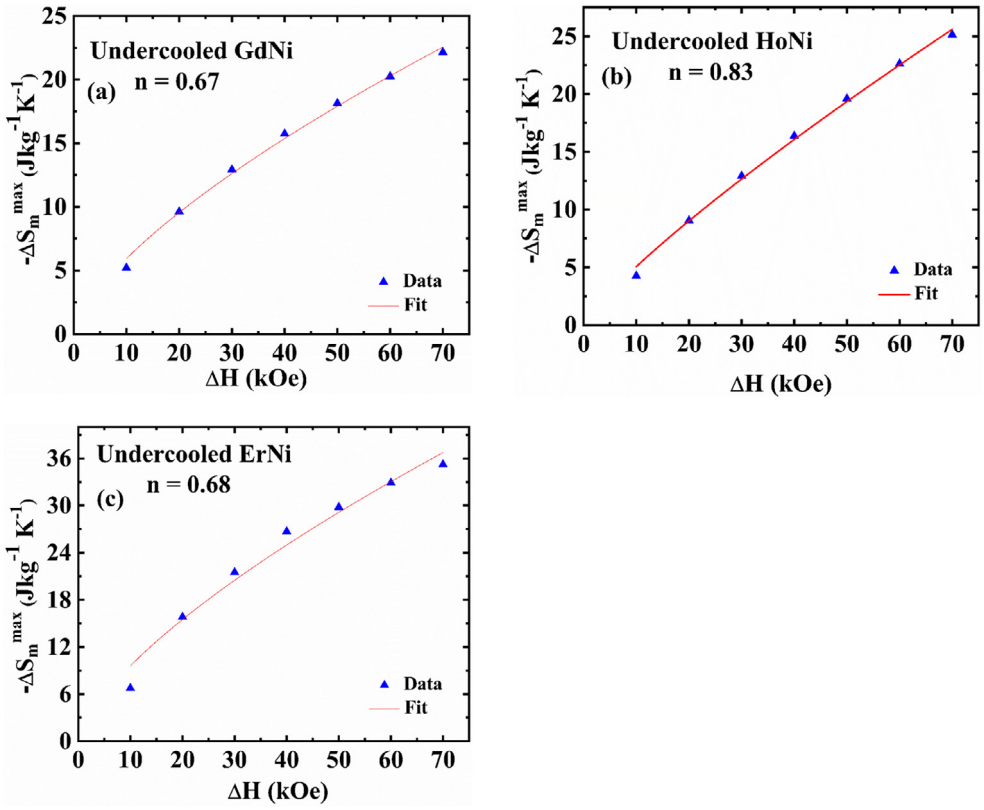

Fig. 6. The power law fit of the magnetic field dependence of the maximum isothermal magnetic entropy change value (ΔS_m^{max} vs ΔH^n).

CRediT authorship contribution statement

Jinu Kurian: Investigation, Formal analysis. **M.R. Rahul:** Investigation. **J. Arout Chelvane:** Resources. **A.V. Morozkin:** Visualization, Formal analysis. **A.K. Nigam:** Investigation. **Gandham Phanikumar:** Resources, Methodology. **R. Nirmala:** Conceptualization, Methodology, Validation, Funding acquisition, Supervision.

Acknowledgements

R. N thanks DST, India for the project support (Sanction no. INT/RUS/RFBR/P-196). J. K. and R. N thank Department of Physics, IITMadras for providing SVSM and FESEM facilities. Authors thank D. Buddhikot, TIFR for the help with low field magnetization measurement.

References

[1] J. Lyubina, R. Schäfer, N. Martin, L. Schultz, O. Gutfleisch, Adv. Mater. 22 (2010) 3735 and references therein.
[2] P.J. Ibarra-Gaytan, C.F. Sanchez-Valdes, J.L. Sanchez Llamazares, Pablo Alvarez-Alonso, Pedro Gorria, J.A. Blanco, Appl. Phys. Lett. 103 (2013) 152401.
[3] J.L. Sánchez Llamazares, C.F. Pablo Álvarez-Alonso, P.J. Sánchez-Valdés, J.A. Blanco Ibarra-Gaytán, Pedro Gorria, Curr. Appl. Phys. 16 (2016) 963.
[4] P. Alvarez-Alonso, C.O. Aguilar-Ortiz, J.P. Camarillo, D. Salazar, H. Flores-Zuniga, V.A. Chernenko, Appl. Phys. Lett. 109 (2016) 212402.
[5] R. Rajivgandhi, J. Arout Chelvane, A.K. Nigam, S.K. Je-Geun Park, Malik, R. Nirmala, J. Magn. Magn. Mater. 418 (2016) 9.
[6] R. Rajivgandhi, J. Arout Chelvane, S. Quezado, S.K. Malik, R. Nirmala, J. Magn. Magn. Mater. 433 (2017) 169.
[7] Aparna Sankar, J. Arout Chelvane, A.V. Morozkin, A.K. Nigam, S. Quezado, S.K. Malik, R. Nirmala, AIP Adv. 8 (2018) 056208.

[8] J. Kurian, J. Arout Chelvane, A.V. Morozkin, A.K. Nigam, S.K. Malik, R. Nirmala, IEEE Trans. Magnetics 54 (2018) 2103004.
[9] Jun-fan Jiang, Hao Ying, Tang-fu Feng, Ren-bing Sun, Xie Li, Fang Wang, Curr. Appl. Phys. 18 (2018) 1605.
[10] P. Kumar, K.G. Suresh, A.K. Nigam, O. Gutfleisch, J. Phys. D. Appl. Phys. 41 (2008) 245006.
[11] D.B. Fahrenheit, Philos. Trans. Roy. Soc. Lond. 39 (1724) 78.
[12] Dieter M. Herlach, Douglas M. Matson (Eds.), Solidification of Containerless Undercooled Melts, Wiley-VCH, Germany, 2012.
[13] S.C. Abrahams, J.L. Bernstein, R.C. Sherwood, J.H. Wernick, H.J. Williams, J. Phys. Chem. Solids 25 (1964) 1069.
[14] F. Izumi, The Rietveld Method, Oxford University Press, Oxford, 1993.
[15] J.A. Blanco, J.R. Fernandez, J.C. Gomez sal, J.R. Carvajal, D. Gignoux, J. Phys. Condens. Matter 7 (1995) 2843.
[16] J.A. Blanco, J.C. Gomez Sal, J.R. Fernandez, D. Gignoux, D. Schmitt, J.R. Carvajal, J. Phys. Condens. Matter 4 (1992) 8233.
[17] K. Sato, S. Iwasaki, K. Mori, Y. Isikawa, J. Magn. Magn. Mater. 31–34 (1983) 207.
[18] Y. Isikawa, K. Mori, K. Sato, M. Ohashi, Y. Yamaguchi, J. Appl. Phys. 55 (1984) 2031.
[19] Nobuyuki Kinami, Hu. Guanghui, Izuru Umehara, JPS Conf. Proc. 3 (2014) 017012.
[20] V.K. Pecharsky, K.A. Gschneidner Jr., Int. J. of Refrig. 29 (2006) 1239.
[21] H. Oesterreicher, F.T. Parker, J. Appl. Phys. 55 (1984) 4336.
[22] V. Franco, J.S. Blázquez, A. Conde, Appl. Phys. Lett. 89 (2006) 222512.
[23] K. Uhlířová, J. Prokleška, J. Poltierová Vejpravová, V. Sechovský, K. Maezawa, J. Magn. Magn. Mater. 310 (2007) 1753.